Phylogenetic and population structure analyses uncover pervasive misclassification and help assessing the biosafety of *Pseudomonas alloputida* for biotechnological applications

Hemanoel Passarelli-Araujo[1,2,*], Sarah H. Jacobs[2], Glória R. Franco[1], Thiago M. Venancio[2,*]

[1]Departamento de Bioquímica e Imunologia, Instituto de Ciências Biológicas, Universidade Federal de Minas Gerais, Belo Horizonte, MG, Brazil

[2]Laboratório de Química e Função de Proteínas e Peptídeos, Centro de Biociências e Biotecnologia, Universidade Estadual do Norte Fluminense Darcy Ribeiro, Campos dos Goytacazes, RJ, Brazil.

*Corresponding authors

Short running title: Population structure of *Pseudomonas alloputida*

Av. Alberto Lamego 2000, P5 sala 217; Parque Califórnia
Campos dos Goytacazes, RJ, Brazil
CEP: 28013-602
HPA: hemanuel.passarelli@gmail.com; TMV: thiago.venancio@gmail.com

Abstract

The *Pseudomonas putida* group comprises strains with biotechnological and clinical relevance. *P. alloputida* was proposed as a new species and highlighted the misclassification of *P. putida*. Nevertheless, the population structure of *P. alloputida* remained unexplored. We retrieved 11,025 *Pseudomonas* genomes and used *P. alloputida* Kh7^{T} to delineate the species. The *P. alloputida* population structure comprises at least 7 clonal complexes (CCs). Clinical isolates are mainly found in CC4 and acquired resistance genes are present at low frequency in plasmids. Virulence profiles support the potential of CC7 members to outcompete other plant or human pathogens through a type VI secretion system. Finally, we found that horizontal gene transfer had an important role in shaping the ability of *P. alloputida* to bioremediate aromatic compounds such as toluene. Our results provide the grounds to understand *P. alloputida* genetic diversity and safety for environmental applications.

Keywords: *Pseudomonas putida group*, *Pseudomonads*, cgMLST

1. Introduction

The genus *Pseudomonas* is diverse and composed of Gram-negative bacteria [1, 2]. Since the first description of *Pseudomonas*, in 1894, the taxonomy of the genus has evolved in parallel with new methodologies to discriminate species [1]. The *Pseudomonas* taxonomy was inconsistent until the division in rRNA homology groups [2]. Nevertheless, because of the limited resolution of the 16S rRNA gene for intra-specific classification, other housekeeping genes were later used to improve taxonomic resolution [3, 4].

The *Pseudomonas putida* group includes other species, such as *P. monteilii*, *P. fulva*, *P. plecoglossicida*, and *P. putida sensu stricto*. Species from this group are ubiquitous in soil and water, and several strains have been isolated from various environments, such as polluted soils and plant roots [5, 6]. *P. putida* species are well known to perform many functions such as plant growth promotion, bioremediation, and protection against plant pathogens [7].

Because of its high metabolic diversity, applications of *P. putida* have been proposed for environmental, industrial, and agricultural uses [5]. Among well-known *P. putida* species, *P. putida* KT2440 is a model organism to study plant-microbe interactions [8, 9]. KT2440 was isolated from garden soil in Japan and has become a workhorse for industrial biotechnology because of its high metabolic versatility, genetic accessibility, and stress-resistance [10]. In addition to the biotechnological application of *P. putida* species, some clinical isolates have been described as reservoirs of resistance genes [11, 12], raising concerns about its biosafety.

53 Recently, Keshavarz-Tohid et al. (2019) showed that *P. putida* KT2440 and other
54 known *P. putida* strains (e.g. BIRD-1, F1, and DOT-T1E) are distant from the type
55 strain *P. putida* NBRC 14164^T and hence should be classified as a member of a novel
56 species, *Pseudomonas alloputida,* whose type strain is Kh7 (=CFBP 8484^T =LMG
57 29756^T) [13]. Here, we report the population structure of *P. alloputida*, which was used
58 to estimate the diversity and distribution of bioremediation and plant growth promotion
59 genes. Further, we used the inferred population structure to better understand the
60 prevalence of antibiotic resistance and virulence genes and to assess, in detail, the
61 potential biosafety concerns regarding this species.

62

63 **2. Results and Discussion**

64 **2.1. Phylogeny and classification of *Pseudomonas alloputida***

65 We obtained 11,025 *Pseudomonas* genomes available in RefSeq in June 2020, out
66 of which 10,457 had completeness greater than 90% according to BUSCO [14]. We
67 computed the pairwise distances between each isolate using mashtree [15] to compute
68 the distance tree of the genus, which is highly diverse (Figure 1). We mapped each
69 genome deposited in the NCBI RefSeq as *P. putida* in the tree and found that the
70 highest density of genomes falls within a monophyletic group of 439 isolates with
71 average nucleotide identity (ANI) values between 84% and 100% (Figure S1a); this
72 clade corresponds to the *P. putida* group (Figure 1) and comprises other species such
73 as *P. plecoglossicida*, *P. monteilli,* and *P. fulva*.

74 ANI analysis provides a raw estimate of bacterial species [16]. A minimum threshold
75 of 95% ANI has been used to attain species membership, a value that has been

76 empirically defined based on correlations with DNA-DNA hybridization and 16S rRNA
77 thresholds [16, 17]. We used *P. alloputida* Kh7^T as an anchor-strain to evaluate the
78 ANI values from other isolates in the *P. putida* group. The sorted distribution of ANI
79 values from Kh7^T showed an abrupt break around 95%, supporting its effectiveness as
80 a threshold to delineate *P. alloputida* (Figure S1b). The isolate previously classified as
81 *P. monteilli* IOFA19 (GCA_000633915.1) had the lowest ANI value within the predicted
82 species (95.48%), followed by a drop to 91.13% (Figure S1b).

83 We conducted a network analysis to assess the species composition according to
84 ANI > 95% with members from the *P. putida* group. We observed a discrete number of
85 cohesive clusters that would correspond to the expected number of species within the
86 *P. putida* group (Figure 2). We retrieved other species such as *P. asiatica*, *P. soli*, and
87 *P. monteilli*, as well as some potentially novel species (Table S1). In this analysis, a
88 species was defined as a cluster containing a type strain and at least three genomes,
89 or a cluster without a type strain, but with at least ten connected genomes. We retrieved
90 the main species from the *P. putida* group and found clusters that most likely
91 correspond to new species (Figure 2). Further, the species number is likely
92 underestimated, as new genomes would increase the number of connections in the
93 network.

94 The poor classification of *P. putida* isolates is a subject of concern. We observed a
95 clear separation of the clusters with type strains for *P. putida* (NBRC 14164^T) and *P.*
96 *alloputida* (Kh7^T) (Figure 2). *P. putida* and *P. alloputida* comprise groups with 16 and
97 68 genomes, respectively (Figure 2, Table S1). The greater number of *P. alloputida*
98 genomes might have an historical explanation. Although the phylogenetic separation
99 of NBRC 14164^T from other main *P. putida* strains has been noticed before [18],

100 KT2440, a *P. alloputida* isolate [13], has also been used to categorize *P. putida*
101 genomes over the years [6, 8, 18].

102 The use of NBRC 14164^{T} to delimit *P. putida sensu stricto* highlights that many well-
103 known *P. putida* genomes belong to other species. Isolates that are well known for
104 their ability to promote plant growth (W618) [19], to oxidize manganese (GB-1) [20],
105 and to damage human tissues (HB3267) [11], are neither *P. putida* nor *P. alloputida*
106 strains, as they belong to different groups in the network. For example, HB3267 was
107 classified as *P. putida* because of its close phylogenetic relationship with the nicotine
108 degrader S16 [21]. HB3267, as well as DLL-E4, SF1, and S11, were proposed as
109 members of a new species, *Pseudomonas shirazica* [13]. However, we found that
110 these strains, along with S16, grouped with *Pseudomonas asiatica* type strain,
111 confirming *P. shirazica* as an heterotypic synonym of *P. asiatica* [22]. Henceforth, we
112 focused our analyses in the novel *P. alloputida* species because of its greater number
113 of genomes and of the presence of key strains associated with bioremediation, plant
114 growth promotion, and biocontrol.

115 **2.2. Pangenome analysis**

116 An effective way to investigate the evolution of a given population is through
117 pangenome analysis. A pangenome is defined as the total set of genes in a given
118 species [23], which is subdivided into core genes, when present in all isolates;
119 accessory genes, when present in at least two (but not in all) isolates or; exclusive
120 genes. By using 68 isolates, the *P. alloputida* pangenome comprises 25,782 gene
121 families, of which 3803 (14.75%) constitute the core genome (i.e. genes present at
122 least 95% of the isolates). By analyzing the slope of the curve (α= 0.417), we inferred
123 that *P. alloputida* has an open pangenome [23] (Figure S2). Our estimated α value is

124 much lower than the maximum threshold used to define an open pangenome ($\alpha < 1$),
125 which is in line with a previous study [24]. Further, this low α value implies high rates
126 of new gene families will be found if more isolates are included in the analysis.

127 The high number of gene families in the *P. alloputida* pangenome is explained by
128 unique and low-frequency genes. Only 6,373 genes families (24.71%) are found
129 between 5% to 95% of the isolates, while 15,606 (60.53%) are found in less than 5%
130 of the isolates, including 10,917 unique genes. The high number of low-frequency
131 genes could be partially attributed to fragmented genomes. However, reference
132 genomes such as DOT-T1E showed 267 unique genes, far more than the average of
133 160.5 unique genes found across the dataset. Although the number of low-frequency
134 genes may be overestimated, the high prevalence of unique genes among closely-
135 related genomes indicates a high turnover of unstable genes that might be adaptive
136 under transient selective pressures in their environments.

137 We also estimated the genomic fluidity (φ) of *P. alloputida*. The φ estimator is a
138 robust metric that represents the ratio of unique gene families to the sum of gene
139 families, averaged over randomly chosen genomes pairs [25]. The smaller the φ, the
140 greater the genes shared by a pair of randomly selected genomes. Analyzing φ instead
141 of the core genome proportion provides a more realistic measure of cohesiveness
142 within a species, particularly because low-frequency genes directly affect the
143 pangenome size. *P. alloputida* has $\varphi = 0.20 \pm 0.04$, indicating that random pairs of *P.*
144 *alloputida* genomes have an average 20% and 80% of unique and shared genes,
145 respectively.

146

147 **2.3. Population structure**

148 Determining relationships between isolates can provide novel insights into the
149 metabolic diversity of a given species. The Multilocus Sequence Typing (MLST)
150 analysis is a technique to characterize genomes based on single-nucleotide
151 polymorphisms (SNPs) within a few housekeeping genes. MLST schemes are
152 available for several species [26]. In an MLST analysis, each combination of SNPs
153 defines a Sequence Type (ST) that can be linked to form Clonal Complexes (CC) [26].
154 A variation of classical MLST is the core genome MLST (cgMLST), which provides
155 greater resolution by using SNPs from the entire core genome [27]. Here, we used
156 225,009 SNPs obtained from the *P. alloputida* core genome to reconstruct the
157 phylogenetic tree and the cgMLST profile.

158 The cgMLST tree unveiled 7 CCs (Figure 3a), out of which CC1 is the most distant
159 from the rest of the population, a trend that is also supported by the ANI analysis
160 (Figure S3). Six out of the 9 clinical isolates were found in CC4 and three in CC7. We
161 also checked whether the same clustering pattern could be obtained by analyzing the
162 presence/absence patterns of accessory genes. We estimated the Jaccard distance
163 for genes present between 5% - 95% of the isolates to perform a Principal Coordinate
164 Analysis (PCoA), which allowed us to resolve all the main groups, particularly CC1,
165 CC4, and CC7 (Figure 3b).

166 We also performed a Discriminant Analysis of Principal Components (DAPC) [28]
167 to recover the genes that contribute most to separate the population based on their
168 presence/absence profiles (Figure S4). The top 50 discriminating genes separate CC5
169 and CC1 from the rest of the population, but fail to resolve the relationships between
170 other CCs (Figure S5). Next, we used branch lengths from cgMLST tree as an indirect

171 estimator of diversity within the CCs (Figure 3c). CC7 is the most clonal group,
172 comprising 9 isolates, including KT2440 and three clinical isolates (GTC_16482,
173 GTC_16473, and NBRC_111121).

174 The MLST scheme for *P. putida* species comprises eight housekeeping genes
175 (*argS, gyrB, ileS, nuoC, ppsA, recA, rpoB,* and *rpoD*) [29]. We assigned isolates to STs
176 and grouped those into CCs (Table S2). This analysis revealed some incongruences
177 with previous reports [29]. For example, by using allele combinations with perfect-
178 match to predict STs, KT2440 was detected as ST69 and not as ST58 [29], indicating
179 that a revision in the public database is warranted. The predicted number of CCs was
180 also supported by the admixture model from STRUCTURE [30]. This model assumes
181 that each isolate has ancestry from one or more *K* genetically different sources, which
182 we referred to as CCs. The number of CCs corresponds to the estimated number of
183 clusters represented by parameter *K*. Instead of using the highest raw marginal
184 likelihood, we followed the protocol for estimating the best *K* value suggested by
185 Evanno et al [31]. The *ad hoc* statistics ΔK indicates that, according to our dataset, the
186 population structure of *P. alloputida* is composed of at least 7 CCs (Figure 3d).

187 Once data from eight *loci* may be insufficient to accurately describe the population
188 structure of *P. alloputida*, the populations identified by STRUCTURE were only
189 considered if they matched cgMLST results. When correlating the cgMLST tree
190 topology with ancestry proportion predicted for each isolate, we observed a clear
191 delimitation of genetic blocks for each CC (Figure 4). However, there are a few
192 inconsistencies. For example, isolate B4 has a greater ancestry proportion with CC2,
193 although cgMLST indicates its greater proximity to CC3. In addition, KCJK7916, FF4,
194 and B6-2 were not assigned to a CC because, although they have a higher proportion

195 of ancestry with CC3, they are paraphyletic to CC3 and CC4. Since CCs are assumed
196 to be monophyletic, these strains were designated as No Clonal Complex (NOCC). We
197 expect that a greater number of *P. alloputida* genomes from isolates from various
198 sources will improve the resolution of the *P. alloputida* population structure, including
199 the CC assignment to isolates described here as NOCC.

200 The cgMLST phylogenetic tree and the distance tree support CC1 as the basally
201 branching group of *P. alloputida* (Figure 4). CC1 comprises isolates from deep-sea
202 sediments from Indian Ocean, costal water from the Pacific Ocean, lotus field, and
203 arthropods (Table 1). The main difference of CC1 is the lack of 229 gene families in
204 the accessory genome, which are present in at least one isolate from all other CCs
205 (Table S3). Among these absent gene families, there is a genomic island with nearly
206 46 Kbp encompassing 38 genes. Some of those genes are involved in sugar transport,
207 as previously identified in KT2440 (CC7) [6], as well as genes encoding hypothetical
208 proteins (coordinates 3,126,465-3,172,496 in KT2440).

209

210 **2.4. Resistance profiles**

211 We evaluated the composition of antibiotic resistance genes using the CARD
212 database [32]. All 15 different genes in the core resistome encode MDR efflux pumps
213 (Table 2, Table S4), including MexAB-OprM, MexEF-OprN, and MexJK, from the
214 resistance-nodulation-cell division (RND) efflux pumps family. These efflux pumps are
215 associated with intrinsic and acquired multidrug resistance in *P. aeruginosa* [33, 34].
216 However, these RND efflux pumps may play an alternative role in *P. alloputida* by
217 pumping out toxic substances such as toluene [35]. We also identified *cpxR*, which

218 encodes a protein that promotes MexAB-OprM expression in the absence of the MexR
219 repressor in *P. aeruginosa* [36], which is absent in *P. alloputida*. The presence of
220 MexAB-OprM in the core genome, under CpxR regulation, supports its involvement
221 with intrinsic physiology in addition to drug resistance, because this complex can be
222 involved in both quorum-sensing and mediation of *P. aeruginosa*-host interaction [37,
223 38].

224 Regarding the acquired resistome, we found 45 different genes that confer
225 resistance by pumping out or inactivating antibiotics, as well as by interacting with
226 antibiotic targets (Table S4). These genes are distributed at low-frequency (Figure 5a),
227 indicating that most of them are strain-specific or acquired through horizontal gene
228 transfer. In general, there is no clear correlation between acquired resistome and
229 population structure (Figure S6), although CC7 has more acquired resistance genes
230 than other CCs (Figure 5c, Figure S6).

231 Our results highlight clinical strains harboring a range of resistance genes. In total,
232 9 out of 68 (13.2%) *P. alloputida* genomes analyzed here belong to clinical strains.
233 Along with efflux pumps, the acquired resistome includes genes encoding antibiotic-
234 inactivating enzymes that confer resistance to beta-lactams (e.g. bla_{CARB-3}, bla_{IMP-1},
235 bla_{OXA-2}, bla_{PDC-7}, bla_{TEM-1}, and bla_{VIM-2}); to aminoglycosides (e.g. *aac(6')-IIa*, *aadA*,
236 *aph(3'')-Ia*, and *aph(6')-Id*; chloramphenicol (*cat*) and; to fosfomycin (*fosA*) (Table S2).
237 These genes were distributed in few strains, mostly clinically relevant (Figure S6, Table
238 S4); the top four strains with more acquired resistance genes were GTC_16473 (19
239 genes), GTC_16482 (16 genes), DZ-F23 (14 genes), and 15420352 (11 genes).
240 Importantly, all of these strains (except DZ-F23) are clinical.

241 We evaluated the presence of acquired genes in plasmids predicted with the PLSDB
242 database (version 2020_06_29) [39]. *P. alloputida* GTC_16473 contained the genes
243 *aac(6')-IIa*, *aadA23*, and bla_{CARB-3} located in a scaffold with high identity with the pJR2
244 plasmid from *Pasteurella multocida* (NC_004772.1). We also identified bla_{OXA-2},
245 *aadA22*, *aac(6')-Ia*, *aac(6')-IIc*, *aph(3'')-Ib*, *aph(6')-Id*, bla_{IMP-1}, and *sul1* genes in
246 plasmid-like sequences in *P. alloputida* GTC_16473 that have not reached the
247 coverage thresholds to be reliably classified as plasmids, supporting an
248 underestimation of plasmids in *P. alloputida* isolates. *P. alloputida* XWY-1 (CC6) also
249 contains a plasmid, pXWY-1 (NZ_CP026333.1), which harbors the resistance genes
250 *sul1*, *aadA2,* and *qacH*. This strain was isolated from rice fields in China. Finding non-
251 clinical strains harboring plasmids with such relevant resistance genes warrants further
252 investigation.

253

254 **2.5. Virulence profiles**

255 We used the VFDB database [40] to assess the *P. alloputida* virulence profiles.
256 Although strains such as KT2440 have been approved as a host-vector system safety
257 level 1 [41], the genetic proximity with animal (*P. aeruginosa*) and plant (*P. syringae*)
258 pathogens reinforces the need to evaluate the biosafety of *P. putida* species. The core
259 virulome of *P. alloputida* contains genes associated with twitching motility, siderophore
260 production (pyoverdine), and alginate biosynthesis (Table S5). Importantly, *P.*
261 *alloputida* lacks key virulence genes usually found in *P. aeruginosa*, such as those
262 encoding exotoxin A, alkaline protease, elastase, rhamnolipid biosynthesis pathway
263 components, phospholipase C, plant cell wall-degrading enzymes, and type III
264 secretion system. Although we have detected genes associated with the type III

265 secretion system in both core (HopAJ2 and HopJ1) and acquired resistome (HopAN1),
266 these genes were experimentally ruled out as virulence factors [42].

267 Most of the alginate regulatory and biosynthesis systems are present in the *P.*
268 *alloputida* core virulome (Table S5). The overproduction of alginate plays an important
269 role in inducing the mucoid morphotype in *P. aeruginosa* during chronic infection [43].
270 However, the transcriptional regulatory gene *algM* (*mucC*), associated with genotypic
271 switching, is absent in *P. alloputida*. Since the lack of AlgM leads to the non-mucoid
272 phenotype in *P. aeruginosa* [8], it can account for the non-mucoid phenotype in *P.*
273 *alloputida* under no water stress conditions. Although the genotypic switching is
274 unlikely to occur in *P. alloputida*, alginate production is important under water stress
275 conditions by promoting biofilm development and protecting from desiccation [44].

276 The acquired virulome comprised genes for type II and VI secretions systems,
277 adherence, and iron uptake (Table S5). While most isolates had a low frequency of
278 resistance genes, the virulence factors displayed a bimodal distribution (Figure 5b), a
279 pattern that has been previously observed for *Klebsiella aerogenes* [45]. Genes from
280 the acinetobactin gene cluster and HSI-I type VI secretion system were differentially
281 distributed across CCs (Figure 6a), although it remains unclear whether these patterns
282 emerged mainly from gene gain or loss. In *Acinetobacter baumannii*, iron uptake is
283 mainly performed by the siderophore acinetobactin [46], which is synthesized by the
284 proteins encoded by the *bauABCDE* operon. We found this operon in *P. alloputida*
285 strains within CC5, CC6, and CC7 (Figure 6a). Further, this operon was surrounded
286 by genes coding for proteins from chemotaxis sensory transducer (PP_2599) and
287 aminotransferases (PP_2588) families (Figure 6b). Siderophore-mediated iron

288 acquisition has been investigated in *P. alloputida* KT2440 [47] (CC7), but the role
289 played by *bauABCDE* in this species is yet to be elucidated.

290 Present in all strains from other CCs, the type VI secretion system (T6SS) HSI-I is
291 absent in CC5 and CC6 (except XWY-1) isolates (Figure 6a). In KT2440 (CC7), HSI-I
292 is a potent weapon against other bacteria (e.g. phytopathogens), increasing the
293 competitiveness of *P. alloputida* [48]. The absence of T6SS virulence genes has been
294 reported for BIRD-1 (CC5) [48], and our work generalizes this observation to all CC5
295 members. In KT2440, T6SS is crucial to kill phytopathogens such as *Xanthomonas*
296 *campestris* [49]. These results indicate that BIRD-1 and other members from CC5 are
297 likely less efficient than KT2440 as biocontrol agents. Moreover, all clinical *P.*
298 *alloputida* strains harbor T6SS, indicating their potential ability to outcompete other
299 bacteria during infections.

300

301 **2.6. Plant growth promotion and bioremediation properties**

302 The ability of *P. putida* species to promote plant growth and bioremediate toxic
303 compounds have been explored [8, 10, 50, 51]. We searched for genes involved in
304 plant growth promotion and bioremediation through a literature search of genes that
305 have already been described for *Pseudomonas* species (Table S6). We found genes
306 in the core genome, such as the pyrroloquinoline quinone-encoding operon
307 *pqqBCDEFG,* associated with mineral phosphate solubilization in *Serratia marcescens*
308 [52] and *Pseudomonas fluorescens* [53] (Table S7). Mineral solubilization has already
309 been reported experimentally for BIRD-1 [50] and KT2440 [53], indicating that all *P.*
310 *alloputida* isolates are genetically equipped to solubilize inorganic phosphate.

311 Another key feature that can enhance plant growth is the colonization of seeds by
312 *P. putida* [54]. In KT2440, genes associated with surface adhesion (e.g. *lapA*, *lapBCD*),
313 flagellum biosynthesis (e.g. *flhB*, *fliF*, *fliD*, *fliC*), and virulence regulation (e.g. *rpoN* and
314 *gacS*) have been experimentally shown to be important for attachment to corn seeds
315 [54]. All these genes, except *lapA* and *fliC*, belongs to the *P. alloputida* core genome
316 (Table S7). Although often described as virulence genes, flagellum genes also play
317 roles in the association of *P. putida* with plants. Other plant growth-promoting genes
318 were also found in the *P. alloputida* accessory genome (Table S7), except for CC1,
319 which lacks all putative plant growth-promoting genes.

320 Many plant growth-promoting bacteria can synthesize phytohormones such as
321 indole-3-acetic acid. *P. alloputida* lacks the main genes involved in this process (e.g.
322 *ipdC*, *iaaM*, and *iaaH*), indicating an incomplete or nonfunctional pathway. Although *P.*
323 *putida* W619 (GCA_000019445.1) is considered one of the most efficient producers of
324 IAA in comparison with other endophytic bacteria [19], this strain belongs to a different
325 species. In addition, *P. alloputida* also lacks AcdS, an enzyme that counteract ethylene
326 stress response, a result that has been experimentally confirmed in KT2440 [55].

327 Besides the ability to promote plant growth, *P. putida* can tolerate or degrade an
328 array of compounds including heavy metals and hydrocarbons. We identified genes in
329 the core genome that allow *P. alloputida* to resist various heavy metals such as copper
330 (*cop* genes) and cobalt/zinc/cadmium (*czcABC*) (Table S8). The copper/silver
331 resistance operon, *cusABC*, was present in the accessory genome. Although we found
332 a wide range of genes associated with bioremediation, there is no clear correlation
333 between the population structure and presence/absence profiles of such genes.

334 *P. putida* is known for its capacity to metabolize aromatic hydrocarbons such as
335 toluene, benzene, and *p*-cymene [6, 8]. The toluene-degrading pathway includes the
336 *todABCDE* operon and the *todST* regulator. The *p*-cymene compound can be
337 degraded by means of the *cymAaAbBCDER* or the *cmtAaAbAcAdBCDEFGHI* operon
338 [56]. We found a genomic island of approximately 48kb long harboring all these genes
339 in F1, DOT-T1E, UV4, UV4/95, YKD221, and NBRC_111125 genomes (Figure S9).
340 All these isolates, except NBRC_111125, were experimentally confirmed to degrade
341 toluene. Further, *P. alloputida* F1 is well-known to grow on toluene [6]; YKD221 was
342 isolated from contaminated industrial soil and degrades *cis*-dichloroethene [57]; DOT-
343 T1E is an isolate known to grow on different carbon sources [58] and; UV4 and UV4/95
344 conduct important industrial biotransformation of arenes, alkenes, and phenols [59].
345 Interestingly, genes in this genomic island presented a very similar genetic context
346 (Figure S7), with an upstream arm-type integrase associated with bacteriophages. We
347 were unable to precisely define the *att* viral sites, indicating a deterioration of the
348 original structure of the putative bacteriophage. Further, the lack of correspondence
349 between population structure and the presence of an integrase upstream the genomic
350 island indicates that this region was likely acquired via independent horizontal gene
351 transfers in distinct *P. alloputida* CCs.

352 We also identified RND efflux pumps involved with solvent tolerance in both core
353 (TtgABC) and accessory genomes (TtgDEF and TtgGHI). TtgABC, TtgDEF, and
354 TtgGHI are required for DOT-T1E to efficiently tolerate toluene [35]. We observed that
355 TtgABC is the same protein-complex predicted as MexAB-OprM, associated with
356 antibiotic resistance in the core genome. This complex extrudes both antibiotics and
357 solvents such as toluene in *P. alloputida* DOT-T1E [35], corroborating the additional
358 and important function to extrude antibiotics and organic solvents in all *P. alloputida*

359 isolates. TtgDEF is located in the same genomic island of *tod* genes. This complex
360 can expel toluene, but not antibiotics [60], reinforcing the variety of molecules that can
361 be extruded by RND efflux pumps and the need to explore the structural basis of this
362 specificity, not only in *P. alloputida* isolates, but also in other bacteria.

363

364 **3. Concluding remarks**

365 Through a remarkable metabolic versatility, *P. putida* species can thrive in a wide
366 variety of niches. In this work, we explored the genetic diversity of *P. alloputida* and
367 characterized its population structure for the first time. Through a large-scale genomic
368 analysis, we identified a major problem with *P. putida species* classification, including
369 several reference strains that likely belong to new species, as also suggested
370 elsewhere [13]. *P. alloputida* has an open pangenome dominated by low-frequency
371 genes. The population structure of this species has at least 7 clonal complexes that
372 were verified by cgMLST and STRUCTURE ancestry simulations. We found that most
373 of the clinical isolates belong to CC4. Together, our results indicate that *P. alloputida*
374 clinical isolates are mainly opportunistic and do not pose considerable health concerns.

375 We analyzed genes of clinical and biotechnological interest. *P. alloputida* has
376 several RND-family efflux pumps that are important to tolerate antibiotics and other
377 toxic compounds such as toluene. The low-frequency acquired resistance genes are
378 predominant in plasmids from a few clinical strains. The detected virulence genes allow
379 *P. alloputida* to synthesize pyoverdine, attach to seed surfaces, and kill other bacteria
380 (including pathogens) through a type VI secretion system. KT2440 is a member of CC7
381 that has the T6SS along with an operon for acinetobactin biosynthesis. *P. alloputida*

382 lacks key genes for the production of indole-3-acetic acid. We also observed that the
383 genes for the degradation of some aromatic compounds, including toluene, were likely
384 horizontally acquired. Our results provide an opportunity for the development of
385 biotechnological applications as well as insights into the genomic diversity of the novel
386 species *P. alloputida*.

387

388 **4. Methods**

389 **4.1. Datasets and genomic features**

390 We recovered 11,025 genomes from the *Pseudomonas* genus in June 2020. To
391 assess the quality of the genomes, we used BUSCO v4.0.6 [14] with a minimum
392 threshold of 90% completeness. The Kh7^{T} (GCA_900291035.1) was used as a
393 reference with mash v.2.2.2 [61] to find genomes with distances up to 0.05. We used
394 mashtree [15] to generate the distance tree. The ANI analysis was performed with
395 pyani 0.2.10 [62]. Network analysis was conducted in R with the igraph package
396 (https://igraph.org). We removed S12 (GCA_000287915.1) and KT2440
397 (GCA_000007565.2) because they were duplicated genomes. Type strains and
398 accession numbers used to define clusters in the network analysis are available in the
399 Table S1. Gene prediction in all isolates was conducted with prokka v1.12 [63] to avoid
400 bias in the identification of protein families. Plasmids were analyzed with PLSD
401 v2020_06_29 [39].

402 **4.2. Pangenome characterization**

403 We inferred the *P. alloputida* pangenome using Roary 3.13.0 [64], with a minimum
404 threshold of 85% identity to cluster proteins. Core genes were defined as those present
405 in more than 95% of the isolates. Jaccard distances were computed by using
406 accessory genes with prevalence between 5% and 95%. Gene content variations
407 between *P. alloputida* ecotypes were inferred with a discriminant analysis of principal
408 components (DAPC) using the *ade4* and *adegenet* packages [28], retaining the 30
409 principal components and 3 discriminant functions. Pangenome openness and fluidity
410 were conducted with micropan [65] with 500 and 1000 permutations, respectively.

411 **4.3. Population structure analysis**

412 We used *in-house* scripts to extract the genes present in all isolates, which were
413 aligned with MAFFT v7.467 [66]. SNPs were retrieved with snp-sites v2.3.3 [67] and
414 SNP alignment was used as input to RAxML v8 [68] to reconstruct the phylogenetic
415 tree using the general time-reversible model and gamma correction. Since we used
416 only variable sites as input, we used ASC_GTRGAMMA to correct ascertainment bias
417 with the Paul Lewis correction. One thousand bootstrap replicates were generated to
418 assess the significance of internal nodes. We inferred the cgMLST scheme using the
419 core genome SNP phylogenetic tree. The phylogenetic tree was visualized with iTOL
420 v4 [69].

421 We downloaded the *P. putida* MLST scheme (on June, 2020) containing 116
422 different STs (https://pubmlst.org/databases/). This scheme was designed for the
423 whole *P. putida* group, not only *P. putida* sensu stricto [29]. We used BLASTN [70] to
424 determine the best-matching MLST allele to access STs. The allelic profile associated
425 with each ST in our dataset was used to conduct population assignment with
426 STRUCTURE v2.3.4 [30] with admixture model. The length of Markov chain Monte

427 Carlo (MCMC) was 50,000, discarding 20,000 iterations as burn-in. The simulations to
428 calculate the parameter K ranged from 2 to 20, with 20 replicates for each K to estimate
429 confidence intervals. Instead of using raw posterior probability to get the best K, we
430 followed the protocol suggested by Evanno, Regnaut and Goudet [31]. Briefly, we
431 calculated the first and second derivatives, resulting in a ΔK of 7. Therefore, we used
432 K = 7 to analyze predicted ancestry probabilities.

433

434 **4.4. Detection of genes associated with antimicrobial resistance, virulence,**
435 **plant growth promotion, and bioremediation**

436 We used the Comprehensive Antimicrobial Resistance Database (CARD) database
437 v3.0.9 [32] to predict antibiotic resistance genes. The virulence factor database (VFDB)
438 [40] was used to determine virulence genes. This database was downloaded on July
439 30 2020 and comprises 28,639 proteins associated with virulence in several
440 pathogens. We used virulence genes previously described for the *Pseudomonas*
441 genus. We clustered proteins based on 70% identity to build a non-redundant database
442 using uclust v1.2.22q [71]. We built the database with plant growth promotion and
443 bioremediation through literature searches (Table S6). All predicted proteins were
444 globally aligned against these databases using usearch v11.0.667 [71] with 50%
445 minimum coverage for query and subject and 60% minimum identity.

446 **Declaration of Competing Interest**

447 The authors declare no conflict of interest.

448 **Acknowledgements**

This work was supported by Fundação Carlos Chagas Filho de Amparo à Pesquisa do Estado do Rio de Janeiro (FAPERJ; grants E-26/203.309/2016 and E-26/203.014/2018), Coordenação de Aperfeiçoamento de Pessoal de Nível Superior - Brasil (CAPES; Finance Code 001), and Conselho Nacional de Desenvolvimento Científico e Tecnológico. The funding agencies had no role in the design of the study and collection, analysis, and interpretation of data and in writing.

REFERENCES

[1] N.J. Palleroni, The Pseudomonas story, Environ Microbiol, 12 (2010) 1377-1383.

[2] R.Y. Stanier, N.J. Palleroni, M. Doudoroff, The aerobic pseudomonads: a taxonomic study, J Gen Microbiol, 43 (1966) 159-271.

[3] L. Ait Tayeb, E. Ageron, F. Grimont, P.A. Grimont, Molecular phylogeny of the genus Pseudomonas based on rpoB sequences and application for the identification of isolates, Res Microbiol, 156 (2005) 763-773.

[4] M. Gomila, A. Pena, M. Mulet, J. Lalucat, E. Garcia-Valdes, Phylogenomics and systematics in Pseudomonas, Front Microbiol, 6 (2015) 214.

[5] D.C. Volke, P. Calero, P.I. Nikel, Pseudomonas putida, Trends Microbiol, 28 (2020) 512-513.

[6] X. Wu, S. Monchy, S. Taghavi, W. Zhu, J. Ramos, D. van der Lelie, Comparative genomics and functional analysis of niche-specific adaptation in Pseudomonas putida, FEMS Microbiol Rev, 35 (2011) 299-323.

[7] K.N. Timmis, Pseudomonas putida: a cosmopolitan opportunist par excellence, Environ Microbiol, 4 (2002) 779-781.

[8] K.E. Nelson, C. Weinel, I.T. Paulsen, R.J. Dodson, H. Hilbert, V.A. Martins dos Santos, D.E. Fouts, S.R. Gill, M. Pop, M. Holmes, L. Brinkac, M. Beanan, R.T. DeBoy, S. Daugherty, J. Kolonay, R. Madupu, W. Nelson, O. White, J. Peterson, H. Khouri, I. Hance, P. Chris Lee, E. Holtzapple, D. Scanlan, K. Tran, A. Moazzez, T. Utterback, M. Rizzo, K. Lee, D. Kosack, D. Moestl, H. Wedler, J. Lauber, D. Stjepandic, J. Hoheisel, M. Straetz, S. Heim, C. Kiewitz, J.A. Eisen, K.N. Timmis, A. Dusterhoft, B. Tummler, C.M. Fraser, Complete genome sequence and comparative analysis of the metabolically versatile Pseudomonas putida KT2440, Environ Microbiol, 4 (2002) 799-808.

478 [9] E. Belda, R.G. van Heck, M. Jose Lopez-Sanchez, S. Cruveiller, V. Barbe, C. Fraser, H.P. Klenk, J.
479 Petersen, A. Morgat, P.I. Nikel, D. Vallenet, Z. Rouy, A. Sekowska, V.A. Martins Dos Santos, V. de
480 Lorenzo, A. Danchin, C. Medigue, The revisited genome of Pseudomonas putida KT2440
481 enlightens its value as a robust metabolic chassis, Environ Microbiol, 18 (2016) 3403-3424.
482 [10] P.I. Nikel, V. de Lorenzo, Pseudomonas putida as a functional chassis for industrial biocatalysis:
483 From native biochemistry to trans-metabolism, Metab Eng, 50 (2018) 142-155.
484 [11] M. Fernandez, M. Porcel, J. de la Torre, M.A. Molina-Henares, A. Daddaoua, M.A. Llamas, A. Roca,
485 V. Carriel, I. Garzon, J.L. Ramos, M. Alaminos, E. Duque, Analysis of the pathogenic potential of
486 nosocomial Pseudomonas putida strains, Front Microbiol, 6 (2015) 871.
487 [12] L. Molina, Z. Udaondo, E. Duque, M. Fernandez, P. Bernal, A. Roca, J. de la Torre, J.L. Ramos,
488 Specific Gene Loci of Clinical Pseudomonas putida Isolates, PLoS One, 11 (2016) e0147478.
489 [13] V. Keshavarz-Tohid, J. Vacheron, A. Dubost, C. Prigent-Combaret, P. Taheri, S. Tarighi, S.M.
490 Taghavi, Y. Moenne-Loccoz, D. Muller, Genomic, phylogenetic and catabolic re-assessment of
491 the Pseudomonas putida clade supports the delineation of Pseudomonas alloputida sp. nov.,
492 Pseudomonas inefficax sp. nov., Pseudomonas persica sp. nov., and Pseudomonas shirazica sp.
493 nov, Syst Appl Microbiol, 42 (2019) 468-480.
494 [14] M. Seppey, M. Manni, E.M. Zdobnov, BUSCO: Assessing Genome Assembly and Annotation
495 Completeness, Methods Mol Biol, 1962 (2019) 227-245.
496 [15] L.S. Katz, T. Griswold, S.S. Morrison, J.A. Caravas, S. Zhang, H.C. den Bakker, X. Deng, H.A. Carleton,
497 Mashtree: a rapid comparison of whole genome sequence files, Journal of Open Source
498 Software, 4 (2019).
499 [16] M. Richter, R. Rossello-Mora, Shifting the genomic gold standard for the prokaryotic species
500 definition, Proc Natl Acad Sci U S A, 106 (2009) 19126-19131.
501 [17] L.M. Bobay, The Prokaryotic Species Concept and Challenges, in: H. Tettelin, D. Medini (Eds.) The
502 Pangenome: Diversity, Dynamics and Evolution of Genomes, Cham (CH), 2020, pp. 21-49.
503 [18] K. Yonezuka, J. Shimodaira, M. Tabata, S. Ohji, A. Hosoyama, D. Kasai, A. Yamazoe, N. Fujita, T.
504 Ezaki, M. Fukuda, Phylogenetic analysis reveals the taxonomically diverse distribution of the
505 Pseudomonas putida group, J Gen Appl Microbiol, 63 (2017) 1-10.
506 [19] S. Taghavi, C. Garafola, S. Monchy, L. Newman, A. Hoffman, N. Weyens, T. Barac, J. Vangronsveld,
507 D. van der Lelie, Genome survey and characterization of endophytic bacteria exhibiting a
508 beneficial effect on growth and development of poplar trees, Appl Environ Microbiol, 75 (2009)
509 748-757.
510 [20] R.A. Rosson, K.H. Nealson, Manganese binding and oxidation by spores of a marine bacillus, J
511 Bacteriol, 151 (1982) 1027-1034.

512 [21] L. Molina, Z. Udaondo, E. Duque, M. Fernandez, C. Molina-Santiago, A. Roca, M. Porcel, J. de la
513 Torre, A. Segura, P. Plesiat, K. Jeannot, J.L. Ramos, Antibiotic resistance determinants in a
514 Pseudomonas putida strain isolated from a hospital, PLoS One, 9 (2014) e81604.
515 [22] M. Tohya, S. Watanabe, T. Tada, H.H. Tin, T. Kirikae, Genome analysis-based reclassification of
516 Pseudomonas fuscovaginae and Pseudomonas shirazica as later heterotypic synonyms of
517 Pseudomonas asplenii and Pseudomonas asiatica, respectively, Int J Syst Evol Microbiol, 70
518 (2020) 3547-3552.
519 [23] H. Tettelin, V. Masignani, M.J. Cieslewicz, C. Donati, D. Medini, N.L. Ward, S.V. Angiuoli, J. Crabtree,
520 A.L. Jones, A.S. Durkin, R.T. Deboy, T.M. Davidsen, M. Mora, M. Scarselli, I. Margarit y Ros, J.D.
521 Peterson, C.R. Hauser, J.P. Sundaram, W.C. Nelson, R. Madupu, L.M. Brinkac, R.J. Dodson, M.J.
522 Rosovitz, S.A. Sullivan, S.C. Daugherty, D.H. Haft, J. Selengut, M.L. Gwinn, L. Zhou, N. Zafar, H.
523 Khouri, D. Radune, G. Dimitrov, K. Watkins, K.J. O'Connor, S. Smith, T.R. Utterback, O. White,
524 C.E. Rubens, G. Grandi, L.C. Madoff, D.L. Kasper, J.L. Telford, M.R. Wessels, R. Rappuoli, C.M.
525 Fraser, Genome analysis of multiple pathogenic isolates of Streptococcus agalactiae:
526 implications for the microbial "pan-genome", Proc Natl Acad Sci U S A, 102 (2005) 13950-13955.
527 [24] Z. Udaondo, L. Molina, A. Segura, E. Duque, J.L. Ramos, Analysis of the core genome and
528 pangenome of Pseudomonas putida, Environ Microbiol, 18 (2016) 3268-3283.
529 [25] A.O. Kislyuk, B. Haegeman, N.H. Bergman, J.S. Weitz, Genomic fluidity: an integrative view of gene
530 diversity within microbial populations, BMC Genomics, 12 (2011) 32.
531 [26] K.A. Jolley, J.E. Bray, M.C.J. Maiden, Open-access bacterial population genomics: BIGSdb software,
532 the PubMLST.org website and their applications, Wellcome Open Res, 3 (2018) 124.
533 [27] M. de Been, M. Pinholt, J. Top, S. Bletz, A. Mellmann, W. van Schaik, E. Brouwer, M. Rogers, Y.
534 Kraat, M. Bonten, J. Corander, H. Westh, D. Harmsen, R.J. Willems, Core Genome Multilocus
535 Sequence Typing Scheme for High- Resolution Typing of Enterococcus faecium, J Clin Microbiol,
536 53 (2015) 3788-3797.
537 [28] T. Jombart, S. Devillard, F. Balloux, Discriminant analysis of principal components: a new method
538 for the analysis of genetically structured populations, BMC Genet, 11 (2010) 94.
539 [29] K. Ogura, K. Shimada, T. Miyoshi-Akiyama, A multilocus sequence typing scheme of Pseudomonas
540 putida for clinical and environmental isolates, Sci Rep, 9 (2019) 13980.
541 [30] J.K. Pritchard, M. Stephens, P. Donnelly, Inference of population structure using multilocus
542 genotype data, Genetics, 155 (2000) 945-959.
543 [31] G. Evanno, S. Regnaut, J. Goudet, Detecting the number of clusters of individuals using the
544 software STRUCTURE: a simulation study, Mol Ecol, 14 (2005) 2611-2620.
545 [32] B.P. Alcock, A.R. Raphenya, T.T.Y. Lau, K.K. Tsang, M. Bouchard, A. Edalatmand, W. Huynh, A.V.
546 Nguyen, A.A. Cheng, S. Liu, S.Y. Min, A. Miroshnichenko, H.K. Tran, R.E. Werfalli, J.A. Nasir, M.

547 Oloni, D.J. Speicher, A. Florescu, B. Singh, M. Faltyn, A. Hernandez-Koutoucheva, A.N. Sharma,
548 E. Bordeleau, A.C. Pawlowski, H.L. Zubyk, D. Dooley, E. Griffiths, F. Maguire, G.L. Winsor, R.G.
549 Beiko, F.S.L. Brinkman, W.W.L. Hsiao, G.V. Domselaar, A.G. McArthur, CARD 2020: antibiotic
550 resistome surveillance with the comprehensive antibiotic resistance database, Nucleic Acids
551 Res, 48 (2020) D517-D525.
552 [33] P.D. Lister, D.J. Wolter, N.D. Hanson, Antibacterial-resistant Pseudomonas aeruginosa: clinical
553 impact and complex regulation of chromosomally encoded resistance mechanisms, Clin
554 Microbiol Rev, 22 (2009) 582-610.
555 [34] H.P. Schweizer, Efflux as a mechanism of resistance to antimicrobials in Pseudomonas aeruginosa
556 and related bacteria: unanswered questions, Genet Mol Res, 2 (2003) 48-62.
557 [35] A. Rojas, E. Duque, G. Mosqueda, G. Golden, A. Hurtado, J.L. Ramos, A. Segura, Three efflux pumps
558 are required to provide efficient tolerance to toluene in Pseudomonas putida DOT-T1E, J
559 Bacteriol, 183 (2001) 3967-3973.
560 [36] Z.X. Tian, X.X. Yi, A. Cho, F. O'Gara, Y.P. Wang, CpxR Activates MexAB-OprM Efflux Pump
561 Expression and Enhances Antibiotic Resistance in Both Laboratory and Clinical nalB-Type Isolates
562 of Pseudomonas aeruginosa, PLoS Pathog, 12 (2016) e1005932.
563 [37] K. Evans, L. Passador, R. Srikumar, E. Tsang, J. Nezezon, K. Poole, Influence of the MexAB-OprM
564 multidrug efflux system on quorum sensing in Pseudomonas aeruginosa, J Bacteriol, 180 (1998)
565 5443-5447.
566 [38] P. Sanchez, J.F. Linares, B. Ruiz-Diez, E. Campanario, A. Navas, F. Baquero, J.L. Martinez, Fitness of
567 in vitro selected Pseudomonas aeruginosa nalB and nfxB multidrug resistant mutants, J
568 Antimicrob Chemother, 50 (2002) 657-664.
569 [39] V. Galata, T. Fehlmann, C. Backes, A. Keller, PLSDB: a resource of complete bacterial plasmids,
570 Nucleic Acids Res, 47 (2019) D195-D202.
571 [40] B. Liu, D. Zheng, Q. Jin, L. Chen, J. Yang, VFDB 2019: a comparative pathogenomic platform with
572 an interactive web interface, Nucleic Acids Res, 47 (2019) D687-D692.
573 [41] L.F.C. Kampers, R.J.M. Volkers, V.A.P. Martins Dos Santos, Pseudomonas putida KT2440 is HV1
574 certified, not GRAS, Microb Biotechnol, 12 (2019) 845-848.
575 [42] A.P. Macho, J. Ruiz-Albert, P. Tornero, C.R. Beuzon, Identification of new type III effectors and
576 analysis of the plant response by competitive index, Mol Plant Pathol, 10 (2009) 69-80.
577 [43] R.L. Henry, C.M. Mellis, L. Petrovic, Mucoid Pseudomonas aeruginosa is a marker of poor survival
578 in cystic fibrosis, Pediatr Pulmonol, 12 (1992) 158-161.
579 [44] W.S. Chang, M. van de Mortel, L. Nielsen, G. Nino de Guzman, X. Li, L.J. Halverson, Alginate
580 production by Pseudomonas putida creates a hydrated microenvironment and contributes to

581 biofilm architecture and stress tolerance under water-limiting conditions, J Bacteriol, 189 (2007)
582 8290-8299.
583 [45] H. Passarelli-Araujo, J.K. Palmeiro, K.C. Moharana, F. Pedrosa-Silva, L.M. Dalla-Costa, T.M.
584 Venancio, Genomic analysis unveils important aspects of population structure, virulence, and
585 antimicrobial resistance in Klebsiella aerogenes, FEBS J, 286 (2019) 3797-3810.
586 [46] W.Y. Song, H.J. Kim, Current biochemical understanding regarding the metabolism of
587 acinetobactin, the major siderophore of the human pathogen Acinetobacter baumannii, and
588 outlook for discovery of novel anti-infectious agents based thereon, Nat Prod Rep, 37 (2020)
589 477-487.
590 [47] S. Matthijs, G. Laus, J.M. Meyer, K. Abbaspour-Tehrani, M. Schafer, H. Budzikiewicz, P. Cornelis,
591 Siderophore-mediated iron acquisition in the entomopathogenic bacterium Pseudomonas
592 entomophila L48 and its close relative Pseudomonas putida KT2440, Biometals, 22 (2009) 951-
593 964.
594 [48] P. Bernal, L.P. Allsopp, A. Filloux, M.A. Llamas, The Pseudomonas putida T6SS is a plant warden
595 against phytopathogens, ISME J, 11 (2017) 972-987.
596 [49] S. Validov, F. Kamilova, S. Qi, D. Stephan, J.J. Wang, N. Makarova, B. Lugtenberg, Selection of
597 bacteria able to control Fusarium oxysporum f. sp. radicis-lycopersici in stonewool substrate, J
598 Appl Microbiol, 102 (2007) 461-471.
599 [50] A. Roca, P. Pizarro-Tobias, Z. Udaondo, M. Fernandez, M.A. Matilla, M.A. Molina-Henares, L.
600 Molina, A. Segura, E. Duque, J.L. Ramos, Analysis of the plant growth-promoting properties
601 encoded by the genome of the rhizobacterium Pseudomonas putida BIRD-1, Environ Microbiol,
602 15 (2013) 780-794.
603 [51] T. Gong, R. Liu, Y. Che, X. Xu, F. Zhao, H. Yu, C. Song, Y. Liu, C. Yang, Engineering Pseudomonas
604 putida KT2440 for simultaneous degradation of carbofuran and chlorpyrifos, Microb Biotechnol,
605 9 (2016) 792-800.
606 [52] F.P. Matteoli, H. Passarelli-Araujo, R.J.A. Reis, L.O. da Rocha, E.M. de Souza, L. Aravind, F.L.
607 Olivares, T.M. Venancio, Genome sequencing and assessment of plant growth-promoting
608 properties of a Serratia marcescens strain isolated from vermicompost, BMC Genomics, 19
609 (2018) 750.
610 [53] S.H. Miller, P. Browne, C. Prigent-Combaret, E. Combes-Meynet, J.P. Morrissey, F. O'Gara,
611 Biochemical and genomic comparison of inorganic phosphate solubilization in Pseudomonas
612 species, Environ Microbiol Rep, 2 (2010) 403-411.
613 [54] E. Duque, J. de la Torre, P. Bernal, M.A. Molina-Henares, M. Alaminos, M. Espinosa-Urgel, A. Roca,
614 M. Fernandez, S. de Bentzmann, J.L. Ramos, Identification of reciprocal adhesion genes in
615 pathogenic and non-pathogenic Pseudomonas, Environ Microbiol, 15 (2013) 36-48.

616 [55] B.R. Glick, B. Todorovic, J. Czarny, Z. Cheng, J. Duan, B. McConkey, Promotion of Plant Growth by
617 Bacterial ACC Deaminase, Critical Reviews in Plant Sciences, 26 (2007).
618 [56] R.W. Eaton, p-Cymene catabolic pathway in Pseudomonas putida F1: cloning and characterization
619 of DNA encoding conversion of p-cymene to p-cumate, J Bacteriol, 179 (1997) 3171-3180.
620 [57] K. Yonezuka, N. Araki, J. Shimodaira, S. Ohji, A. Hosoyama, M. Numata, A. Yamazoe, D. Kasai, E.
621 Masai, N. Fujita, T. Ezaki, M. Fukuda, Isolation and characterization of a bacterial strain that
622 degrades cis-dichloroethenein the absence of aromatic inducers, J Gen Appl Microbiol, 62 (2016)
623 118-125.
624 [58] C. Daniels, P. Godoy, E. Duque, M.A. Molina-Henares, J. de la Torre, J.M. Del Arco, C. Herrera, A.
625 Segura, M.E. Guazzaroni, M. Ferrer, J.L. Ramos, Global regulation of food supply by
626 Pseudomonas putida DOT-T1E, J Bacteriol, 192 (2010) 2169-2181.
627 [59] T. Skvortsov, P. Hoering, K. Arkhipova, R.C. Whitehead, D.R. Boyd, C.C.R. Allen, Draft Genome
628 Sequences of Pseudomonas putida UV4 and UV4/95, Toluene Dioxygenase-Expressing
629 Producers of cis-1,2-Dihydrodiols, Genome Announc, 6 (2018).
630 [60] G. Mosqueda, J.L. Ramos, A set of genes encoding a second toluene efflux system in Pseudomonas
631 putida DOT-T1E is linked to the tod genes for toluene metabolism, J Bacteriol, 182 (2000) 937-
632 943.
633 [61] B.D. Ondov, T.J. Treangen, P. Melsted, A.B. Mallonee, N.H. Bergman, S. Koren, A.M. Phillippy,
634 Mash: fast genome and metagenome distance estimation using MinHash, Genome Biol, 17
635 (2016) 132.
636 [62] L. Pritchard, H.R. Glover, S. Humphris, J.G. Elphinstone, I.K. Toth, Genomics and taxonomy in
637 diagnostics for food security: soft-rotting enterobacterial plant pathogens, Anal. Methods, 8
638 (2016) 10-24.
639 [63] T. Seemann, Prokka: rapid prokaryotic genome annotation, Bioinformatics, 30 (2014) 2068-2069.
640 [64] A.J. Page, C.A. Cummins, M. Hunt, V.K. Wong, S. Reuter, M.T. Holden, M. Fookes, D. Falush, J.A.
641 Keane, J. Parkhill, Roary: rapid large-scale prokaryote pan genome analysis, Bioinformatics, 31
642 (2015) 3691-3693.
643 [65] L. Snipen, K.H. Liland, micropan: an R-package for microbial pan-genomics, BMC Bioinformatics,
644 16 (2015) 79.
645 [66] K. Katoh, D.M. Standley, MAFFT multiple sequence alignment software version 7: improvements
646 in performance and usability, Mol Biol Evol, 30 (2013) 772-780.
647 [67] A.J. Page, B. Taylor, A.J. Delaney, J. Soares, T. Seemann, J.A. Keane, S.R. Harris, SNP-sites: rapid
648 efficient extraction of SNPs from multi-FASTA alignments, Microb Genom, 2 (2016) e000056.
649 [68] A. Stamatakis, RAxML version 8: a tool for phylogenetic analysis and post-analysis of large
650 phylogenies, Bioinformatics, 30 (2014) 1312-1313.

[69] I. Letunic, P. Bork, Interactive Tree Of Life (iTOL) v4: recent updates and new developments, Nucleic Acids Res, 47 (2019) W256-W259.

[70] S.F. Altschul, T.L. Madden, A.A. Schaffer, J. Zhang, Z. Zhang, W. Miller, D.J. Lipman, Gapped BLAST and PSI-BLAST: a new generation of protein database search programs, Nucleic Acids Res, 25 (1997) 3389-3402.

[71] R.C. Edgar, Search and clustering orders of magnitude faster than BLAST, Bioinformatics, 26 (2010) 2460-2461.

660 **Tables**

661 **Table 1.** *Pseudomonas alloputida* isolates used in this study with average nucleotide

662 identity (ANI) from Kh7^{T}.

Strain	Classified as	ANI	CC	Location	Source	Accession
15420352	*P. putida*	0.97	CC4	China	urine	GCA_013305625.1
B2017	*P. putida*	0.97	CC3	Spain	root	GCA_007279645.1
B4	*P. putida*	0.97	CC3	China	soil	GCA_003671955.1
B6-2	*P. putida*	0.97	NOCC	-	soil	GCA_000226035.3
BIRD-1	*P. putida*	0.99	CC5	Spain	rhizosphere	GCA_000183645.1
CA-3	*P. putida*	0.97	CC4	Ireland	waste material	GCA_002810225.1
CY06	*P. monteilii*	0.96	CC1	China	shrimp	GCA_002835905.1
DOT-T1E	*P. putida*	0.97	CC3	Spain	wastewater	GCA_000281215.1
DPA1	*P. putida*	0.97	CC4	Greece	soil	GCA_002891885.1
DZ-F23	*P. putida*	0.95	CC1	China	fly	GCA_002094775.1
F1	*P. putida*	0.97	CC2	USA	soil	GCA_000016865.1
FDAARGOS_409	*P. putida*	0.97	CC4	USA	blood	GCA_002554535.1
FF4	*Pseudomonas sp.*	0.97	NOCC	Chile	wastewater	GCA_007049805.1
FW305-E2	*P. putida*	0.97	CC2	USA	groundwater	GCA_900095365.1
FW305-E2_1	*Pseudomonas sp.*	0.97	CC2	USA	groundwater	GCA_002901725.1
GTC_16473	*Pseudomonas sp.*	0.97	CC7	Japan	*Homo sapiens*	GCA_001753855.1
GTC_16482	*Pseudomonas sp.*	0.97	CC7	Japan	*Homo sapiens*	GCA_001319995.1
H	*P. putida*	0.97	CC7	Germany	soil	GCA_001077495.1
Idaho	*P. putida*	0.98	CC6	China	-	GCA_000226475.2
INSali382	*P. putida*	0.98	CC6	Portugal	vegetable	GCA_001653615.1
IOFA1	*P. putida*	0.96	CC1	Indian Ocean	sediment	GCA_001293025.1
IOFA19	*P. monteilii*	0.95	CC1	Indian Ocean	sediment	GCA_000633915.1
JB	*P. putida*	0.99	CC5	Czech Republic	soil	GCA_001767335.1
JLR11	*P. putida*	0.97	CC7	Spain	wastewater	GCA_001183585.1
JR16	*P. putida*	0.99	CC5	India	soil	GCA_004519745.1
JY-Q	*Pseudomonas sp.*	0.97	CC4	China	tabaco extract	GCA_001655295.1
KB3	*P. putida*	0.96	CC1	Poland	soil	GCA_004614175.1
KBS0802	*Pseudomonas sp.*	0.97	CC7	USA	soil	GCA_005937845.2
KCJK7911	*P. putida*	0.97	CC3	USA	water	GCA_003053335.1
KCJK7916	*P. putida*	0.97	NOCC	USA	water	GCA_003053385.1
KH-18-2	*P. putida*	0.96	CC1	Pacific Ocean	water	GCA_002906815.1
KH-20-11	*P. putida*	0.95	CC1	Pacific Ocean	water	GCA_002906795.1
Kh14	*Pseudomonas sp.*	1.00	CC5	Iran	rhizosphere	GCA_900291005.1
Kh7	*Pseudomonas sp.*	1.00	CC5	Iran	rhizosphere	GCA_900291035.1
KT-90	*P. putida*	0.96	CC1	Pacific Ocean	coastal water	GCA_002906755.1
KT2440	*P. putida*	0.97	CC7	Japan	rhizosphere	GCA_900167985.1
LD6	*P. putida*	1.00	CC5	China	rhizosphere	GCA_003586135.1
LF54	*P. putida*	0.96	CC1	Japan	lotus field	GCA_000390005.2
LS46	*P. putida*	0.97	CC4	Canada	water	GCA_000294445.2
N1R	*P. putida*	0.99	CC5	USA	soil	GCA_900156185.1
NBRC_111118	*Pseudomonas sp.*	0.97	CC4	Japan	*Homo sapiens*	GCA_001320085.1
NBRC_111121	*Pseudomonas sp.*	0.97	CC7	Japan	sputum	GCA_001320165.1

NBRC_111125	*Pseudomonas sp.*	0.97	CC4	Japan	urine	GCA_001320295.1
NBRC_111136	*Pseudomonas sp.*	0.97	CC4	Japan	urine	GCA_001320745.1
NBRC_111139	*Pseudomonas sp.*	0.97	CC4	Japan	eye discharge	GCA_001753955.1
NCTC13185	*P. putida*	0.97	CC7	-	-	GCA_901482375.1
NCTC13186	*P. putida*	0.97	CC7	-	-	GCA_900636645.1
ND6	*P. putida*	0.97	CC2	China	wastewater	GCA_000264665.2
ODNR4SY	*P. putida*	0.97	CC2	USA	water	GCA_009905395.1
OR45a	*P. putida*	0.99	CC5	Poland	activated sludge	GCA_004614155.1
P11	*P. hunanensis*	0.97	CC4	China	high-arsenic soil	GCA_002910975.1
PaW85-2019	*P. putida*	0.97	CC7	Estonia	-	GCA_011750655.1
PaW85-d13TA	*P. putida*	0.97	CC7	Estonia	-	GCA_011750675.1
PCL1760	*P. putida*	1.00	CC5	Spain	rhizosphere	GCA_001282125.1
PD1	*P. putida*	0.97	CC3	USA	root	GCA_000799625.1
RW4053	*Pseudomonas sp.*	0.99	CC5	Germany	river sediments	GCA_003184135.1
S12	*P. putida*	1.00	CC5	Netherlands	soil	GCA_000495455.2
SJTE-1	*P. putida*	0.97	CC2	China	soil	GCA_000271965.2
SMT-1	*Pseudomonas sp.*	0.97	CC7	China	soil	GCA_003204195.1
SWI36	*Pseudomonas sp.*	0.97	CC6	USA	soil	GCA_002948105.1
SWI36_1	*Pseudomonas sp.*	0.98	CC6	USA	soil	GCA_004153505.1
SWI36_2	*Pseudomonas sp.*	0.98	CC6	USA	soil	GCA_004153435.1
TRO1	*P. putida*	0.97	CC4	Denmark	activated sludge	GCA_000367825.1
UV4	*P. putida*	0.97	CC4	UK	laboratory strain	GCA_002165695.1
UV4_95	*P. putida*	0.97	CC4	UK	laboratory strain	GCA_002165665.1
XWY-1	*Pseudomonas sp.*	0.97	CC6	China	rice fields	GCA_002953115.1
YKD221	*P. putida*	0.97	CC2	Japan	soil	GCA_000787655.1
ZKA3	*P. plecoglossicida*	0.98	CC6	Greece	water	GCA_003633555.1

Table 2. Frequency of resistance mechanisms categories in both core and accessory resistome.

Pangenome division	Resistance mechanism	Frequency
Core	Antibiotic efflux	15 genes* (100%)
Accessory	Antibiotic efflux	126 genes (67.74%)
	Antibiotic inactivation	47 genes (25.27%)
	Antibiotic target alteration	3 genes (1.61%)
	Antibiotic target protection	1 gene (0.54%)
	Antibiotic target replacement	9 genes (4.84%)

*Number of different genes.

667 **Figures**

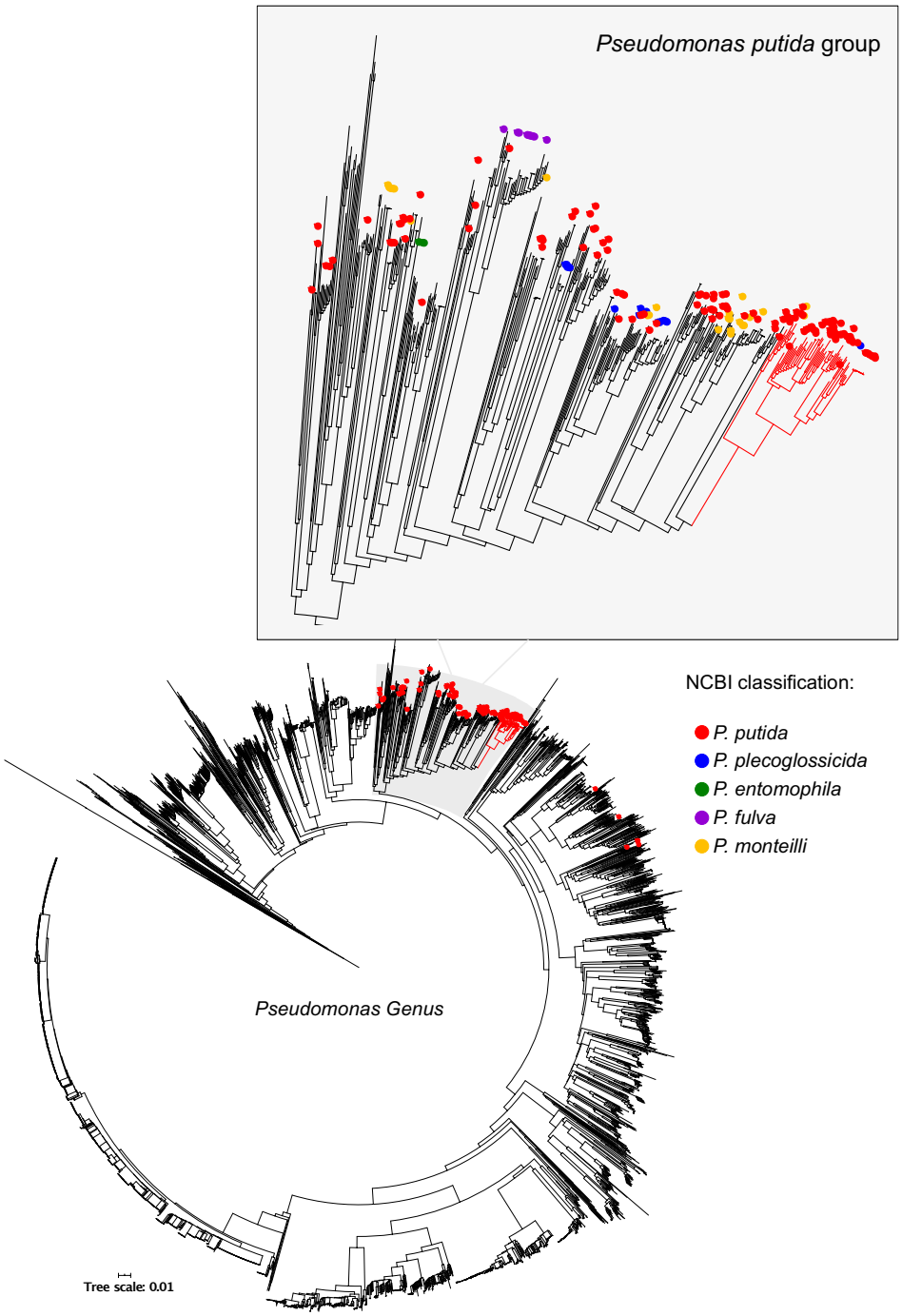

668

669 **Figure 1.** Distance tree of 10,457 *Pseudomonas* genomes from *Pseudomonas* genus.
670 Genomes classified as *P. putida* according to NCBI are marked as red circle. *P. putida*
671 group was highlighted to assess the distribution of misclassified genomes. *P. alloputida*
672 branches are colored in red.

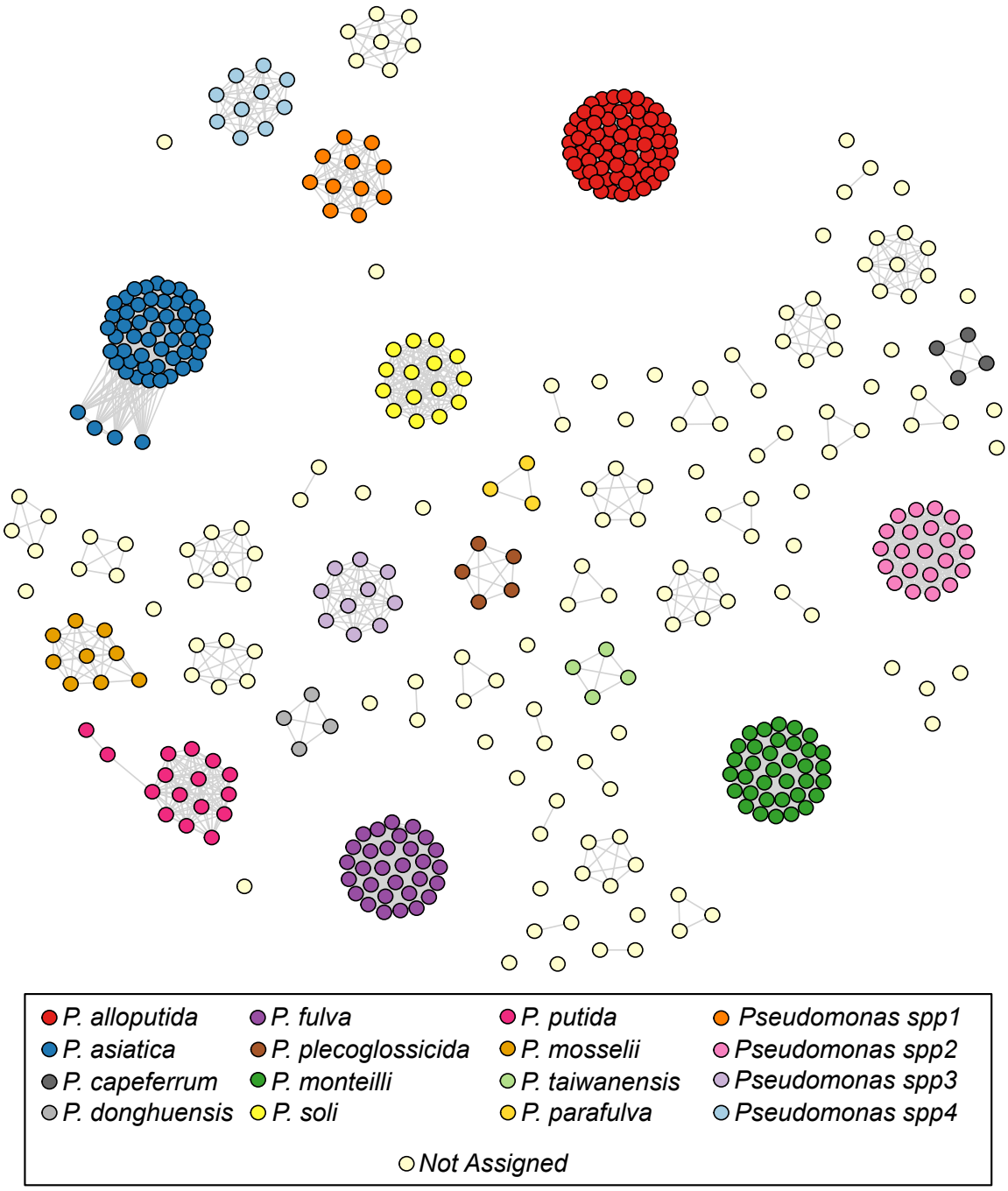

Figure 2. Network analysis of isolates from the *P. putida* group. Nodes represent isolates and edges connect isolates with at least 95% of average nucleotide identity. Clusters with type strains or at least ten genomes were highlighted, as they represent either known or potentially novel species.

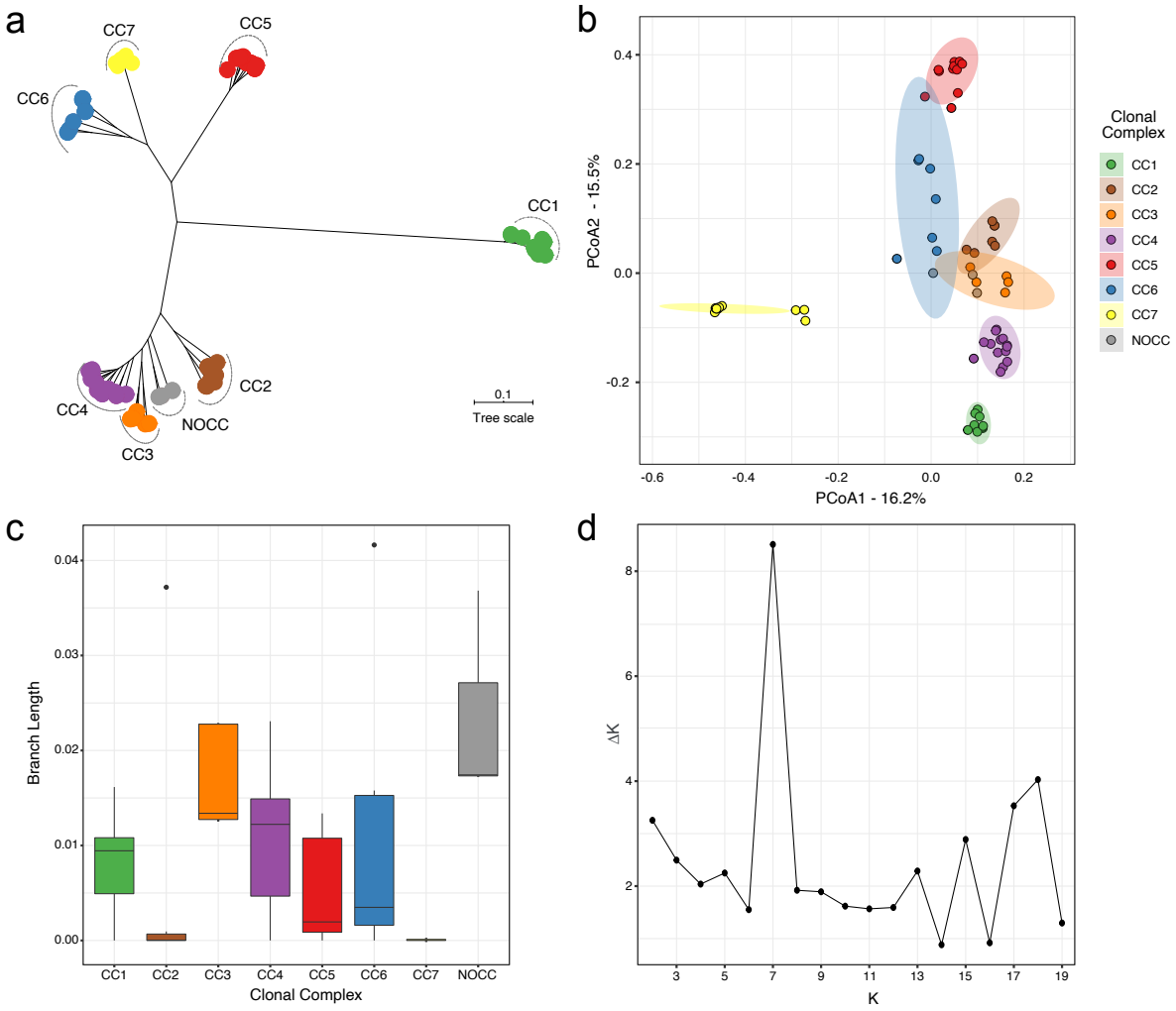

678

679 **Figure 3.** Population structure of *P. alloputida*. **a.** phylogenetic reconstruction using SNPs
680 extracted from core genome to assign the cgMLST scheme. Colors represent distinct Clonal
681 Complexes and NOCC stands for No Clonal Complex assigned with high confidence. **b.**
682 Principal Component Analysis based on the presence/absence profile of accessory genes
683 present in 5% to 95% of the isolates. **c.** Branch lengths for each Clonal Complex. **d.** ΔK
684 distribution to estimate the best value for K, which supports the presence of 7 *P. alloputida*
685 CCs.

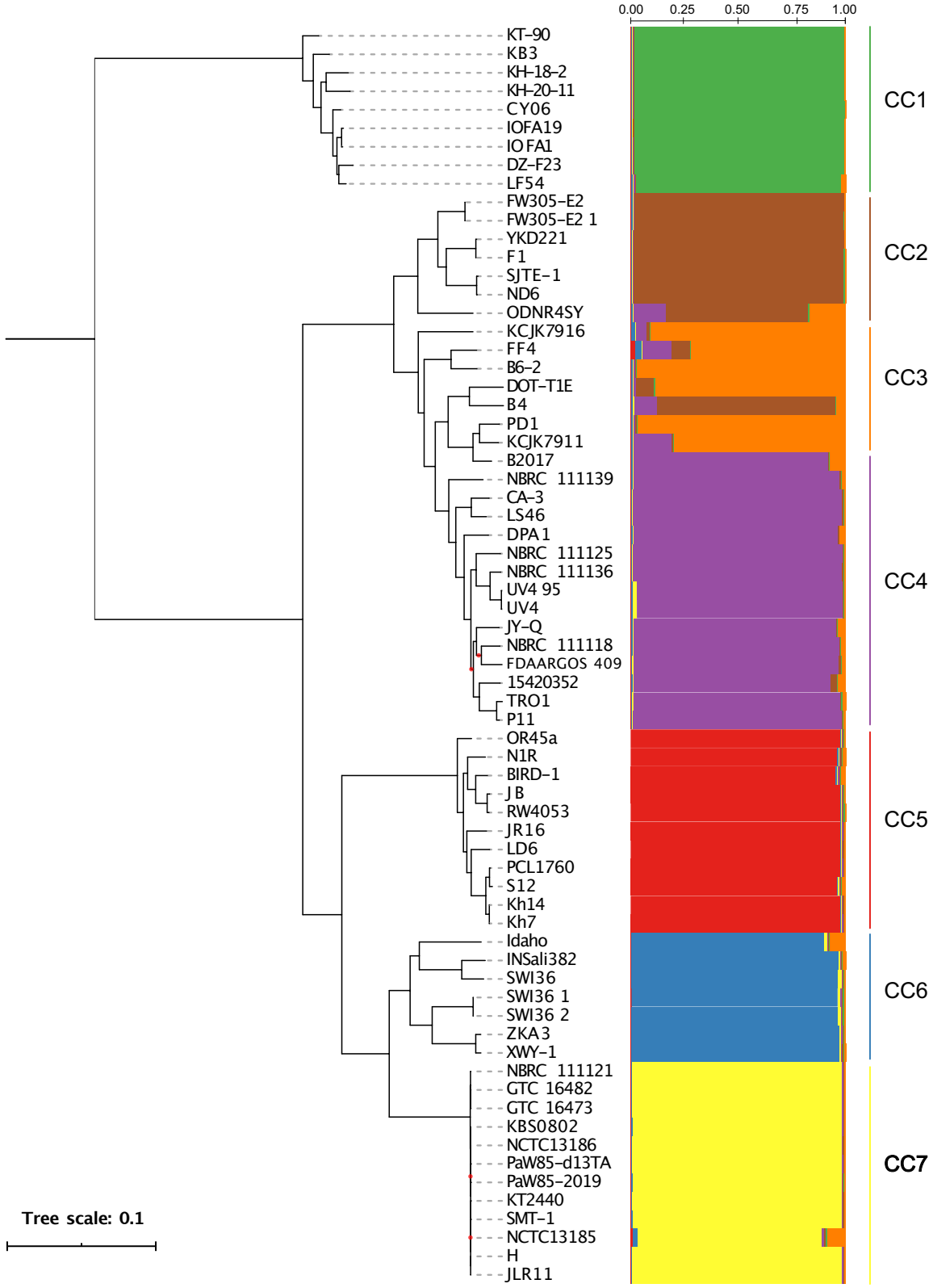

Figure 4. Phylogenetic tree and coancestry barplots correlating the phylogenetic tree using SNPs extracted from core genome and coancestry probabilities assigned with STRUCTURE. Red dots in branches represent bootstrap values lower than 70%. Each color represents one of the seven predicted Clonal Complexes (CC).

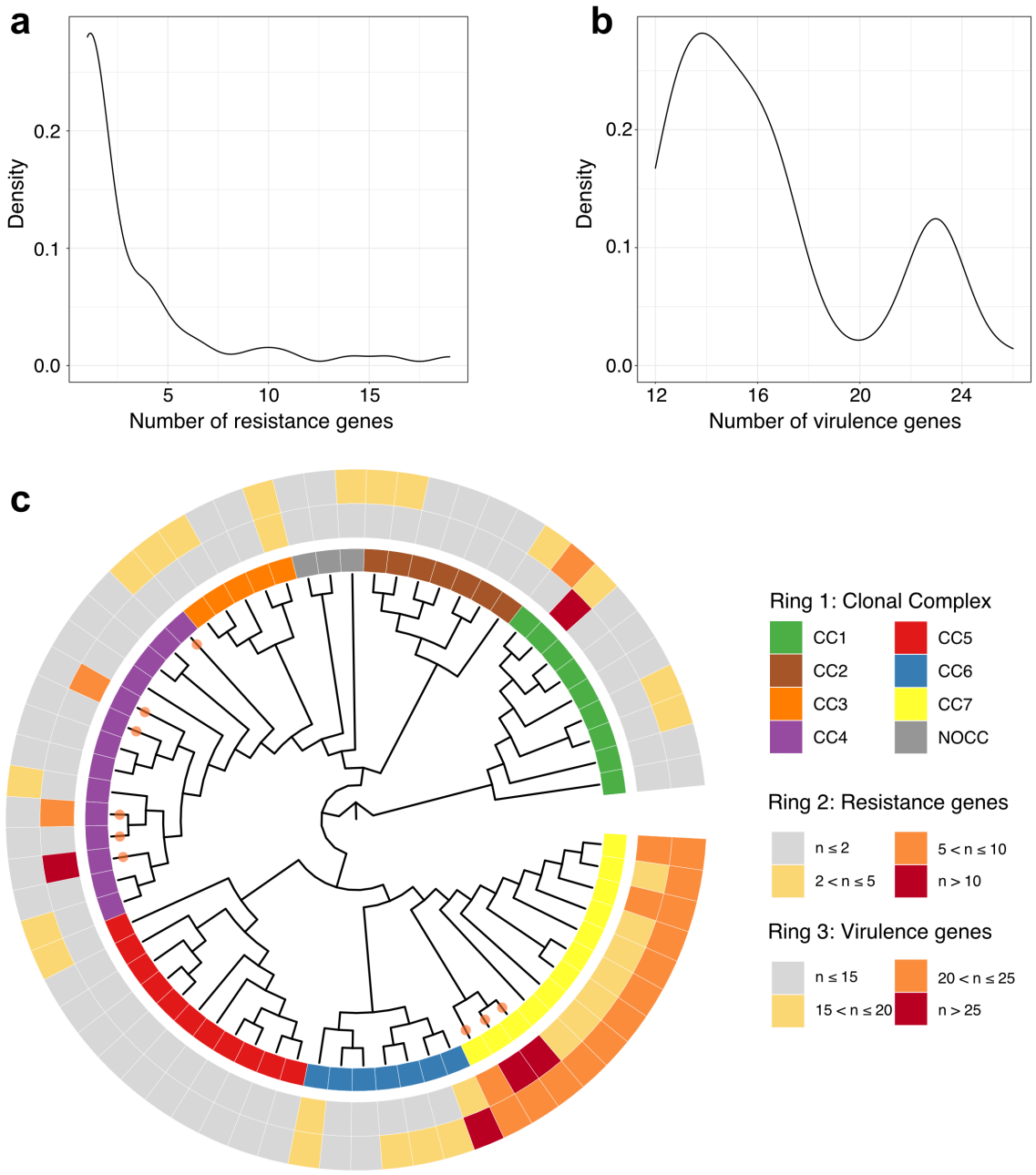

Figure 5. Population structure and distribution of virulence and resistance genes. **a, b.** distribution of acquired resistance and virulence genes. **c.** Maximum likelihood tree from SNPs present in the core genome inferred with 68 genomes used in this study. Branches from clinical isolates are marked with an orange circle. The inner ring represents the clonal complexes (NOCC: "No Clonal Complex"). The second and third rings indicate the number (n) of acquired resistance and virulence genes, respectively.

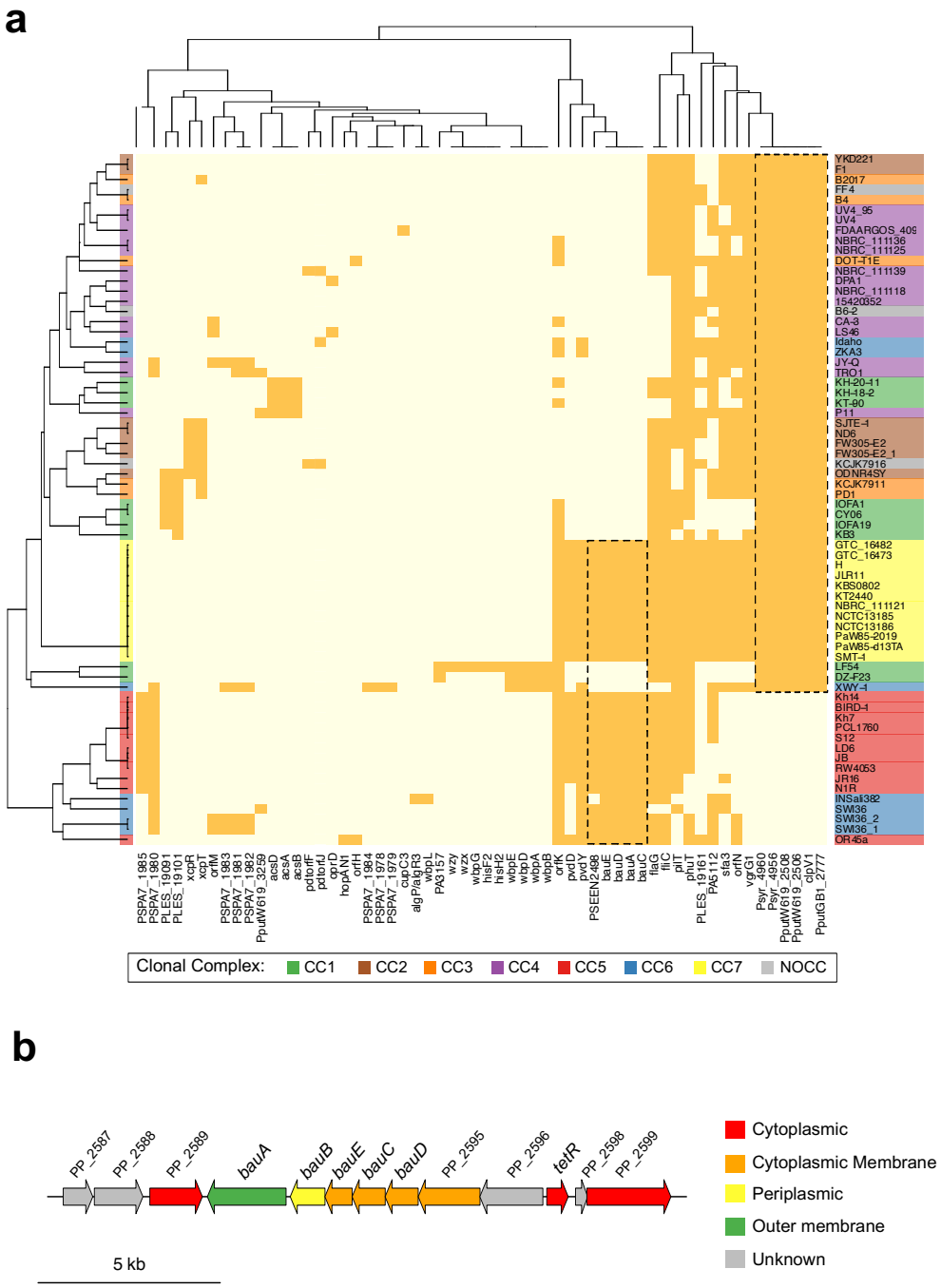

Figure 6. Acquired virulome composition. **a.** Matrix with presence (dark squares) and absence (light squares) profiles of virulence genes. Rows represent strains colored based on Clonal Complex that they belong. Columns are virulence genes identified. **b.** *P. alloputida* KT2440 *bauABCDE* genetic context annotated according Pseudomonas Genome Database (www.pseudomonas.com) and Song and Kim (2020).